Controlling the Growth and Differentiation of Human Mesenchymal Stem Cells by the Arrangement of Individual Carbon Nanotubes

Seon Namgung,[†] Ku Youn Baik,[§] Juhun Park,[†] and Seunghun Hong[†,‡,*]

[†]Department of Physics and Astronomy, Seoul National University, Seoul, 151-747, Korea, [‡]Interdisciplinary Program in Nano-Science and Technology, Department of Biophysics and Chemical Biology, Seoul National University, Seoul, 151-747, Korea, and [§]Plasma Bioscience Research Center, Kwangwoon University, Seoul 139-701, Korea

ABSTRACT Carbon nanotube (CNT) networks on solid substrates have recently drawn attention as a means to direct the growth and differentiation of stem cells. However, it is still not clear whether cells can recognize individual CNTs with a sub-2 nm diameter, and directional nanostructured substrates such as aligned CNT networks have not been utilized to control cell behaviors. Herein, we report that human mesenchymal stem cells (hMSCs) grown on CNT networks could recognize the arrangement of individual CNTs in the CNT networks, which allowed us to control the growth direction and differentiation of the hMSCs. We achieved the directional growth of hMSCs following the alignment direction of the individual CNTs. Furthermore, hMSCs on aligned CNT networks exhibited enhanced proliferation and osteogenic differentiation compared to those on randomly oriented CNT networks. As a plausible explanation for the enhanced proliferation and osteogenic differentiation, we proposed mechanotransduction pathways triggered by high cytoskeletal tension in the aligned hMSCs. Our findings provide new insights regarding the capability of cells to recognize nanostructures smaller than proteins and indicate their potential applications for regenerative tissue engineering.

KEYWORDS: carbon nanotube · human mesenchymal stem cell · recognition of cellular environment · control of cell behaviors · osteogenic differentiation

Human mesenchymal stem cells (hMSCs) are multipotent stem cells which can be differentiated into multiple lineages according to the surrounding environments.[1−7] Recently, nanostructured substrates have been extensively studied to control the growth and differentiation of hMSCs often without any chemical supplements.[8−10] For example, the differentiation of hMSCs was controlled simply by modulating the disorder or the dimension of nanostructures, and the degree of the differentiation in those cases was similar to that in the cases where soluble cues were used.[9,10] However, for those applications, it is often critical to control the growth direction as well as differentiation of the hMSCs.[11−14] For example, the alignment of differentiated bone-cells and secreted collagen can enhance the mechanical strength of bone structures.[15−17] Although various one-dimensional structures have been utilized for that purpose, they were larger than tens of nanometers and thus might cause some disturbance to surrounding biosystems under *in vivo* environments. On the other hand, carbon nanotubes (CNTs) have drawn attention for stem cell engineering[18−20] and were expected to generate minimum disturbance to the surrounding biosystems due to the small diameter of CNTs. However, CNT-based directional substrates such as aligned CNT networks have not been utilized to control the growth direction or differentiation of stem cells, and it is not known whether cells can even recognize individual CNTs. Herein, we report that hMSCs could recognize the arrangement of individual CNTs, which allowed us to control the growth direction and differentiation of the hMSCs without differentiation media. We achieved the directional growth of hMSCs along the alignment direction of the individual CNTs. Significantly, hMSCs on the aligned CNT networks exhibited enhanced proliferation and osteogenic differentiation. We also found the upregulation of genes related to the mechanotransduction pathways, which support that the enhanced proliferation and osteogenic differentiation might be attributed to high cytoskeletal tension in the stretched hMSCs.

Figure 1a displays our experimental procedure to reveal the effect of CNT alignment

* Address correspondence to seunghun@snu.ac.kr.

Received for review June 22, 2011 and accepted August 5, 2011.

Published online August 05, 2011
10.1021/nn2023057

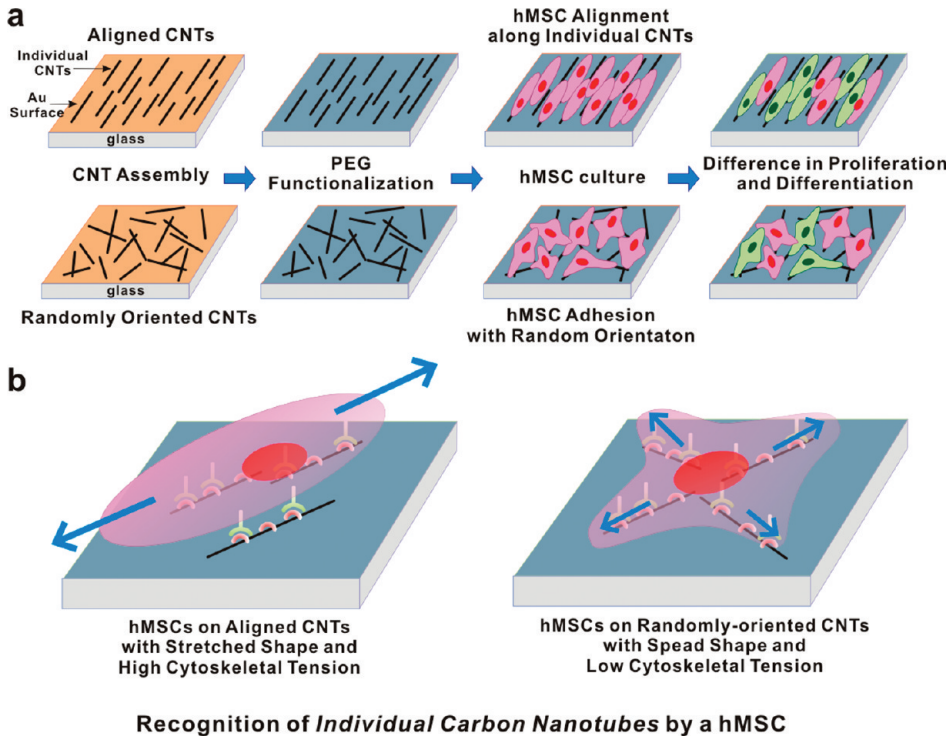

Figure 1. Growth and differentiation of hMSCs on CNT networks with the different arrangement of individual CNTs. (a) Schematic diagram showing the experimental procedure. CNTs were assembled on Au substrates with a low surface density in an aligned or a randomly oriented formation. Then, bare surface regions between the CNTs were functionalized with thiolated polyethylene glycol (PEG-SH). hMSCs were cultured on the substrates, and their growth and differentiation were investigated. (b) Plausible model to explain the hMSC responses to the aligned and the randomly oriented CNT networks. The hMSCs on the aligned CNT networks elongated along the alignment direction of the CNTs because of a high affinity between CNTs and cells. High cytoskeletal tension was induced in the stretched hMSCs on the aligned CNT networks.

in CNT networks on hMSC behaviors. First, to assemble CNT networks in an aligned formation, a few drops of CNT suspensions were applied on spinning Au substrates (Figure S1 in Supporting Information). This process resulted in CNT networks with individual CNTs aligned along the radial direction of the spinning. On the other hand, CNTs were assembled in a randomly oriented formation on Au substrates simply by dipping the substrates in CNT suspensions. The concentration of the CNT suspensions and the dipping time were adjusted to achieve identical CNT surface densities in both of the aligned and the randomly oriented CNT networks. The surface densities of the CNTs in both cases were in the range of 0.7−1.5 CNTs/μm^2. In this range, individual CNTs adsorbed on the substrates were separated from each other. The bare surface regions between the adsorbed CNTs were functionalized with thiolated polyethylene glycols (mPEG-SH), resistant to cell adhesion, to maximize the effect of the individual CNTs on cells. Finally, we cultured hMSCs on the prepared substrates and compared their behaviors on the aligned CNT networks with those on the randomly oriented CNT networks.

Figure 1b shows the plausible mechanism of different cell behaviors depending on the arrangement of individual CNTs in CNT networks. Previous reports showed that cell adhesion proteins, such as fibronectins, had a strong affinity to CNTs, which induced the formation of focal adhesion contacts on the CNTs and selective cell growth on the CNTs.[21] Therefore, if cells could sense individual CNTs and form adhesion contacts on the CNTs, cells would adhere and grow following the direction of the individual CNTs. In this case, we can expect that cells on the aligned CNT networks would stretch along the alignment direction of individual CNTs, while those on the randomly oriented ones would just spread out in random orientations. In addition, different cell shapes drawn by the arrangement of the underlying CNTs might induce different cytoskeletal tension to the hMSCs, which should affect the proliferation and osteogenic differentiation of the hMSCs, probably, *via* cascading mechanotransduction pathways.

RESULTS AND DISCUSSION

Figure 2 panels a and b show AFM topography images of individual CNTs in the aligned and the randomly oriented CNT networks, respectively. Note the individual CNTs in the aligned CNT networks (Figure 2a) were aligned along the radial direction of the spin-coating. The individual CNTs appeared well-separated from each other, which was critical in testing if cells can recognize the individual CNTs.

The distribution of the diameter and the length of the CNTs in the aligned CNT networks are shown in

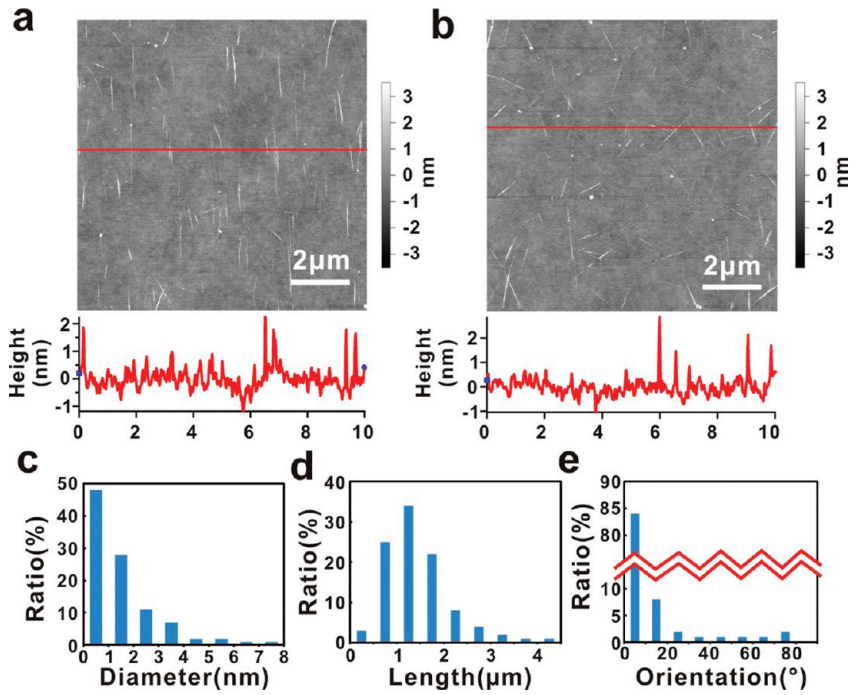

Figure 2. Carbon nanotubes adsorbed on Au substrates in an aligned or a randomly oriented formation. (a) AFM topography image of aligned CNT networks assembled by the spin-coating method (top) and its height profile along the red line in the AFM image (bottom). (b) AFM topography image of the randomly oriented CNT networks (top) and its height profile along the red line in the AFM image (bottom). (c) Histogram of the diameter of the CNTs in the aligned CNT networks. The diameters of 100 CNTs were measured by AFM. The averaged diameter of the CNTs was 1.6 nm. (d) Histogram of the length of individual CNTs in the aligned CNT networks. The lengths of 100 CNTs were measured by AFM. The averaged length of the CNTs was 1.5 μm. (e) Histogram of the orientation of individual CNTs in the aligned CNT networks. The orientation of an individual CNT was defined as the absolute value of an angle between the direction of the CNT and the radial direction of the spin-coating. The orientations of 100 CNTs were measured by AFM.

Figure 2 panels c and d, respectively. The averaged diameter and length of the CNTs in the aligned CNT networks were estimated as 1.6 nm and 1.5 μm, respectively. It should be noted that 70% or more CNTs had a diameter smaller than 2 nm, corresponding to a diameter of a single CNT, which indicates most of the CNTs were separated individually without forming bundles.

The orientation of individual CNTs in the aligned CNT networks was measured with respect to the radial direction of CNT spin-coating, and its distribution was shown in Figure 2e. Note that 80% or more CNTs were aligned along the radial direction with the deviation less than 10°. It indicates that the spin coating procedure allowed us to prepare the aligned CNT networks with a high degree of alignment of the individual CNTs over a large surface area.[22]

We cultured hMSCs on the aligned and the randomly oriented CNT networks to investigate whether the arrangement of the individual CNTs in the CNT networks affected the cell behaviors (Figure 3). Over the surface region as large as 2 cm, hMSCs on the aligned CNT networks were found to grow along the radial directions (marked by white arrows in Figure 3a) which correspond to the alignment directions of individuals CNTs in the aligned CNT networks prepared by the spin-coating method. On the other hand, the hMSCs on the randomly oriented CNT networks were rather aggregated and spread randomly (Figure 3b). Statistical analysis shows that about 70% of hMSCs on the aligned CNT networks were aligned within 20° from the alignment directions of the individual CNTs (Figure 3c). Such an alignment of cells following the arrangement of individual CNTs was also observed for other cells such as NIH3T3 fibroblasts (Figure S2 in Supporting Information). Considering that the diameter of individual CNTs was smaller than 2 nm and the surface density of the CNTs was low, it is quite striking that cells could recognize the individual CNTs and grow following the alignment direction of the CNTs.

Figure 3d shows the fluorescence image of actin filaments in the hMSCs on the aligned CNT networks. Actin filaments in the hMSCs were also found to be aligned along the alignment direction of the individual CNTs. The alignment of actin filaments induced the stretched shape of the hMSCs, which might result in higher cytoskeletal tension. The actin filaments of hMSCs grown on randomly oriented CNT networks were also shown in Figure S3 in Supporting Information. The scanning electron microscope (SEM) image in Figure 3e shows the filopodial extensions of the hMSCs were following the alignment direction of the underlying CNTs. A SEM image with a large scale is also

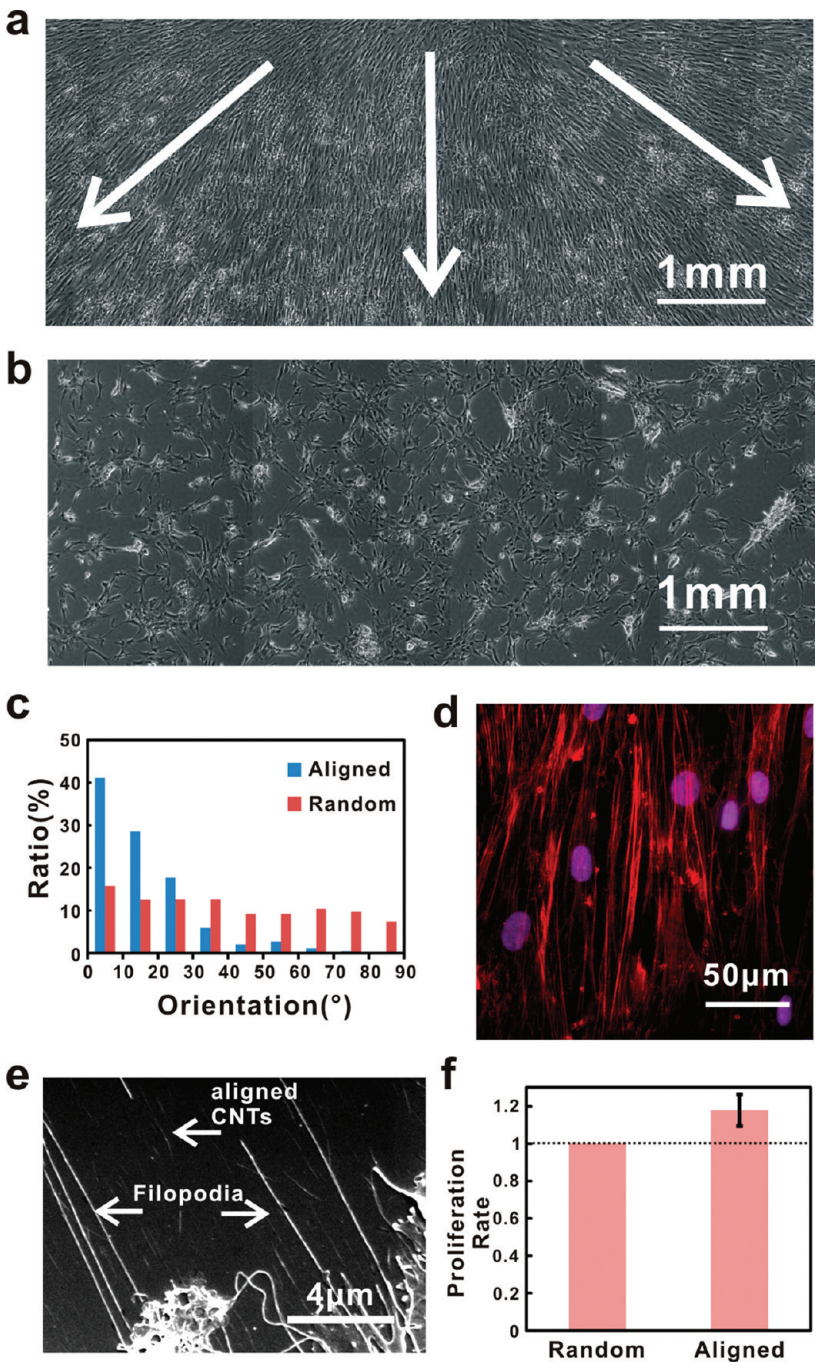

Figure 3. Adhesion and proliferation of hMSCs on aligned or randomly oriented CNT networks. (a) Large area phase contrast image of hMSCs cultured on the aligned CNT networks for 2 weeks. Here, 10 images were combined to reconstruct a single image to show the hMSC growth over a large surface area. The white arrows indicate the radial direction of the CNT spin coating. (b) Large area phase contrast image of hMSCs cultured on the randomly oriented CNT networks for 2 weeks. Ten images were combined to reconstruct a single image to show the hMSC growth over a large surface area. (c) Histogram of the orientation of the hMSCs cultured on the aligned and the randomly oriented CNT networks. The orientation of a hMSC on the aligned CNT networks was defined as an absolute value of the angle between the direction of the long axis of the hMSC and the radial direction of CNT spin coating, while that on the randomly oriented CNT networks was defined as an absolute value of the angle between the direction of the long axis of the hMSC and a fixed direction in microscope images. (d) Fluorescence image of aligned actin filaments in the hMSCs elongated along the aligned CNTs. The actin filaments and nuclei of the hMSCs were stained with TRITC-phalloidins (red) and DAPI (violet), respectively. (e) Scanning electron microscope (SEM) image of the filopodial extensions of the hMSCs cultured on the aligned CNT networks. (f) Proliferation rates analyzed by relative absorbance at 490 nm in the MTS assay. The proliferation rate of hMSCs on the aligned CNT networks was higher than that on the randomly oriented CNT networks ($n = 4$, $p < 0.05$). Here, statistical significance was determined by Student's t test.

shown in Figure S4 in Supporting Information. Filopodial extensions are the assembly of actin filaments at the leading edges of cells, which sense and navigate the environment.[23] The filopodial extension following

the aligned CNTs indicates the high affinity between cells and CNTs as proposed in our mechanism (Figure 1b).

We performed the MTS (3-(4,5-dimethylthiazol-2-yl)-5-(3-carboxymethoxyphenyl)-2-(4-sulfophenyl)-2*H*-tetrazolium, inner salt) assay to study the proliferation of hMSCs on aligned and randomly oriented CNT networks (Figure 3f). The viability of the hMSCs on the aligned CNT networks was enhanced by ~20% compared to that on the randomly oriented CNT networks. This result indicates the arrangement of individual CNTs could affect the proliferation of the cells.

We performed control experiments to reveal key factors inducing the aligned growth of hMSCs on the aligned CNT networks. First, we grew cells on the substrate with only PEG patterns without CNTs (Figure S5 in Supporting Information). In this experiment, aligned CNT networks with PEG passivation were prepared (Figure 1a) and, then, CNTs were removed by sonication leaving only PEG patterns (Figure S5a in Supporting Information). In this case, the hMSCs grew in random directions (Figure S5b in Supporting Information). Previously, it was reported that cell adhesion proteins on CNTs had an activity even better than those on bare glass, and they induced selective and stable cell adhesion onto the CNTs.[21] Our results indicate that the high cell affinity to CNTs played a crucial role for the alignment of hMSCs. Furthermore, we also grew hMSCs on aligned CNT networks without PEG passivation, which resulted in the hMSC growth in random directions (Figure S5c in Supporting Information). These results show that the large difference in cell affinities between CNTs and PEG patterns is required for the alignment of hMSCs.

In addition, we cultured hMSCs on aligned CNT networks with various surface densities of CNTs (Figure S6 in Supporting Information). On the substrates with a surface density of ~0.3 CNT/μm^2, hMSCs did not grow well due to the high coverage of PEG molecules. Interestingly, on substrates with a high surface density of CNTs of over 3 CNTs/μm^2, the hMSCs were distributed randomly disregarding the alignment of the individual CNTs even on the aligned CNT networks. This finding suggests the alignment of hMSCs on the aligned CNT networks depends on the surface density of the individual CNTs in the networks. In the process of cell growth and migration, the protrusions at the leading edge of a cell, such as lamellipodia and filopodia, determine the direction of cell polarity and migration.[23−26] In the advancement process of the protrusions, nascent adhesion complexes first extend for the distance of ~0.25 μm from the cell edges and mature further into focal complexes, focal adhesion sites, and fibrillar adhesions.[26] In our experiments, since the affinity of the adhesion proteins to CNTs was higher than that to PEG, the adhesion sites should be preferentially formed on the CNTs. In case of the low density CNT networks, CNTs with an average length of 1.5 μm were distributed on glass substrates with a surface density of ~1 CNT/μm^2. Thus, the average distance between adjacent CNTs would be larger than ~0.5 μm, which is much larger than the distance between neighboring adhesion complexes of ~0.25 μm. In this case, once a nascent adhesion complex at a part of cell edge was formed on a CNT, the following adhesion complex could not be extended to other CNTs due to the large separation between individual CNTs (Figure 3e and Figure S7a in Supporting Information). Thus, a successive adhesion complex should be formed on the same CNT, and cell growth should follow the directions of the individual CNTs. However, on the substrates with the high surface density of CNTs of ~3 CNTs/μm^2, the closest distance between adjacent CNTs could be at most ~0.17 μm, which is smaller than the scale of the nascent adhesion complex. Therefore, the adhesion complexes could mature without being confined to the individual CNTs, and consequently the cells grew in random directions (Figure S7b in Supporting Information).

Further, we investigated if the arrangement of the individual CNTs could affect the osteogenic differentiation of hMSCs (Figure 4). Figure 4 panels a and b show the immunofluorescence images of osteogenic markers, osteocalcin (OCN) and osteopontin (OPN), in the hMSCs on the aligned and the randomly oriented CNT networks, respectively. The hMSCs were cultured for 4 weeks in cell culture media without osteogenic supplements. To analyze the osteogenic differentiation quantitatively, we performed the quantitative real-time polymerase chain reaction (qPCR) analysis for osteogenic markers including OCN, OPN, alkaline phosphatase (ALP), and core binding factor alpha1 (CBFA1) (Figure 4c). The results of the qPCR experiments showed that the osteogenic markers were up-regulated in the hMSCs on the aligned CNT networks compared to those on the randomly oriented CNT networks, indicating the enhanced osteogenic differentiation of hMSCs on the aligned CNT networks.

We also performed extensive qPCR analysis to explore the underlying mechanism explaining the enhanced osteogenic differentiation of the hMSCs on the aligned CNT networks (Figure 4d,e). Previous work showed that the cytoskeletal tension induced by stretched cell shape or mechanical stimuli activated mechanotransduction pathways, including adhesion-mediated signaling or noncanonical Wnt signaling, to promote osteogenic differentiation.[27−33] The activation of focal adhesion kinase (FAK) in the adhesion-mediated signaling and the formation of Wnt complex in the noncanonical Wnt signaling activate Rho family of GTPases member A (RhoA) and its effector Rho-associated coiled-coil protein kinase (ROCK), resulting in increased cytoskeletal tension in a positive feedback manner.[27−30] The RhoA-ROCK pathway further triggers mitogen-activated protein kinase (MAPK) signaling to

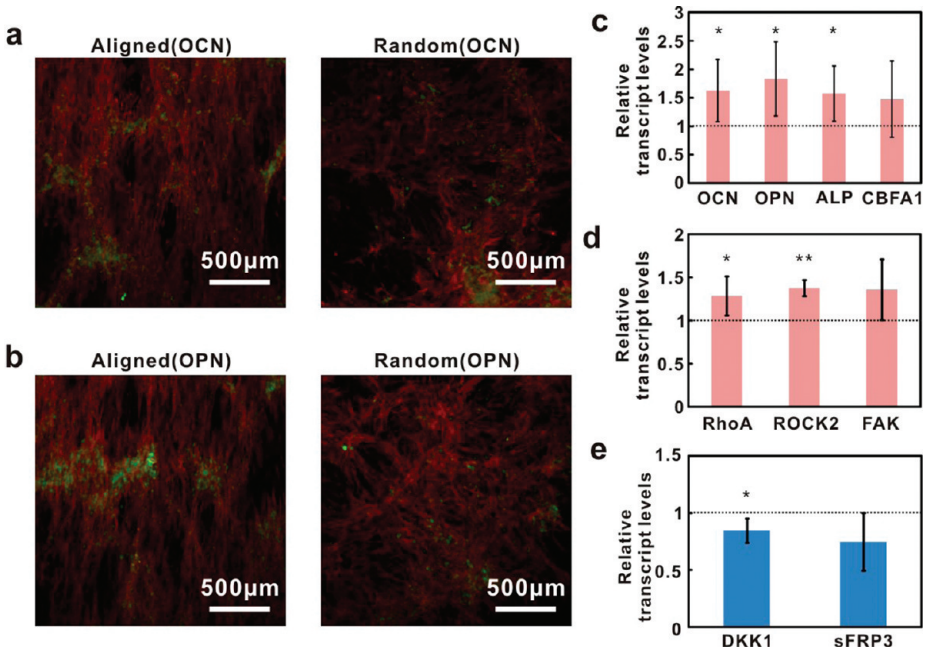

Figure 4. Enhanced osteogenic differentiation of hMSCs on aligned CNT networks through mechanotransduction pathways. hMSCs were cultured on aligned and randomly oriented CNT networks for 4 weeks. (a) Immunofluorescence images of osteocalcins (OCNs, green) in hMSCs on the aligned (left) and the randomly oriented (right) CNT networks. The actin filaments of the hMSCs were stained with TRITC−phalloidins (red). (b) Immunofluorescence images of osteopontins (OPNs, green) in hMSCs on the aligned (left) and the randomly oriented (right) CNT networks. The actin filaments of the hMSCs were stained with TRITC−phalloidins (red). (c) Expression levels of osteogenic genes, including OCN, OPN, alkaline phosphatase (ALP), and core binding factor alpha1 (CBFA1), in the hMSCs on the aligned CNT networks relative to those on the randomly oriented ones. Here, the expression levels of the genes were obtained using qPCR ($n = 3$). (d) Expression levels of the genes involved in the mechanotransduction pathways, including focal adhesion kinase (FAK), Rho family of GTPases member A (RhoA), and Rho-associated coiled-coil protein kinase (ROCK), in the hMSCs on the aligned CNT networks relative to those on the randomly oriented ones. Here, the expression levels of the genes were obtained using qPCR ($n = 3$). (e) Expression levels of the genes of Wnt-antagonists, including dikkopf-1 (DKK1) and secreted frizzled-related protein type 3 (sFRP3), in the hMSCs on the aligned CNT networks relative to those in the hMSCs on the randomly oriented ones. Here, the expression levels of the mRNAs were obtained using qPCR ($n = 3$). Statistical significances were determined by Student's t test: (*) $p < 0.1$; (**) $p < 0.05$.

promote osteogenic differentiation.[27] In our works, we observed the up-regulation of RhoA, ROCK2, and FAK in the hMSCs on the aligned CNT networks compared to those on the randomly oriented ones (Figure 4d). We also observed the down-regulation of dikkopf-1 (DKK1) and secreted frizzled-related protein type 3 (sFRP3), which inhibit the Wnt pathway to suppress osteogenesis,[27] in the hMSCs on the aligned CNT networks compared to those on the randomly oriented ones (Figure 4e). In our experiments, the hMSCs on the aligned CNT networks showed more stretched shape following the alignment direction of the aligned CNT networks compared to those on the randomly oriented ones. In this case, we can expect higher cytoskeletal tension in the more stretched cells on the aligned CNT networks, which should have activated mechanotransduction pathways to promote osteogenic differentiation. Also, note that since RhoA-ROCK pathway and FAK promote the progression of cell cycle,[30,34] the up-regulation of RhoA, ROCK2 and FAK can also explain the enhanced proliferation of hMSCs on the aligned CNT networks as shown in Figure 3f.

In summary, we demonstrated that hMSCs could recognize individual CNTs in CNT networks, and the alignment of the individual CNTs can affect the growth and differentiation of the hMSCs. The hMSCs on the aligned CNT networks were stretched along the alignment direction of the individual CNTs in the networks. Significantly, we observed the enhanced proliferation and osteogenic differentiation of the hMSCs on the aligned CNT networks compared to those on the randomly oriented CNT networks. We found the up-regulation of genes involved in the mechanotransduction pathways in the hMSCs on the aligned CNT networks. It supports our hypothesis that the enhanced proliferation and osteogenic differentiation was caused by the mechanotransduction pathways triggered by the high cytoskeletal tension in the elongated hMSCs on the aligned CNT networks. The recognition of the individual CNTs, even with a sub-2-nm diameter, by hMSCs provides us a new insight into the sensitivity of cell response to surrounding environments. Furthermore, our works can provide an important guideline for various future applications such as designing cell-nanostructure hybrid systems for regenerative tissue engineering. For example, although the biocompatibility of CNTs is still under study, one strategy to apply our method for tissue engineering might be

coating the aligned CNT networks on biocompatible implant substrates. Such substrates should induce the directional growth and enhanced osteogenic differentiation of hMSCs.

EXPERIMENTAL METHODS

Preparation of CNT-Assembled Substrates. Cover glasses were cleaned with piranha solution (H_2SO_4/H_2O_2 = 3:1). A 5 nm thick Ti layer and a 10 nm Au layer were deposited thermally on the cover glasses. Single-walled CNTs (Hanhwa Nanotech) in a powder form were dispersed in *o*-dichlorobenzene (0.005 mg/mL) by sonication. To assemble CNTs in an aligned formation, CNTs in the suspensions were spin-coated on the Au substrates at 5000 rpm. To assemble CNTs in a randomly oriented formation, the Au substrates were placed in the CNT suspensions, rinsed with *o*-dichlorobenzene vigorously and dried with N_2 gas. We adjusted the concentration of CNT suspensions and the dipping time to match the surface density of the CNTs in the randomly oriented CNT networks with that in the aligned CNT networks. The Au surface of the substrates were functionalized with mPEG-SH (mw 750, Rapp Polymere) solution in ethanol (5 mg/mL) for 2 days. The samples were imaged by the AFM system (MFP-3D, Asylum Research) in intermittent mode to measure the diameter, length, orientation, and surface density of the CNTs.

Cell Culture and Imaging. hMSCs from human bone marrow (Lonza) were expanded in MSC growth medium (MSCGM) and used for our experiments at passage 4–6. The prepared substrates were treated with fibronectins (Sigma) in phosphate buffered saline solution (PBS, Gibco) with a concentration of 10 μg/mL for 10 min. The cells were seeded on the substrates with a density of 5000 cells/cm^2 and grown in culture media, high glucose Dulbecco's Modified Eagle Medium (DMEM, Gibco) supplemented with 10% fetal bovine serum (FBS, Gibco) and 1% penicillin–streptomycin (Gibco). The cells were maintained at 37 °C in 5% CO_2 environment and culture media was changed twice a week. The phase contrast images were taken by a Nikon Eclipse TE2000-U microscope with electron multiplying charge coupled device (EMCCD, DQC-FS, Nikon). The morphology and orientation of cells were analyzed by NIS Elements AR imaging software. NIH3T3 fibroblasts were grown with the same procedures as described above.

Imaging Cells by a Scanning Electron Microscope. hMSCs were fixed with 2.5% paraformaldehyde and 2.5% glutaraldehyde in a neutral 0.1 M PBS. The fixatives were warmed to reduce cell shrinkage. Postfixation was performed with 1% osmium tetroxide dissolved in PBS. Samples were treated in graded ethanol series, dried in critical point dryer (SCP-II, Hitachi), coated with platinum using a sputter coater (SCD 005, BAL-TEC), and observed under a field emission scanning electron microscope (SUPRA 55VP, Carl Zeiss).

Immunohistochemistry. hMSCs were fixed in 4% formaldehyde solution, permeabilized with 0.1% Triton X-100, and then blocked with 1% BSA for 1 h. For staining osteogenic markers, cells were incubated with antibodies of osteocalcin (OCN) (1:100, OC4–30, QED Bioscience) or antibodies of osteopontin (OPN) (1:100, AKm2A1, Santa Cruz Biotechnology) for 1 h and then incubated with FITC-conjugated antimouse IgG (1:100, sigma) for 1 h. The actin filaments were stained by TRITC-conjugated phalloidin (1:100, Molecular Probes). For nuclei staining, Prolong gold antifade reagent with DAPI (Invitrogen) was applied. Fluorescence images were obtained using a Nikon Eclipse TE2000-U microscope with electron multiplying charge coupled device (EMCCD, DQC-FS, Nikon).

Cell Proliferation Assay. Cells were seeded on the aligned and the randomly oriented CNT networks with an identical density. The proliferation rate of the cells was determined by the MTS assay using CellTiter 96 Aqueous One Solution Cell Proliferation Assay (Promega) according to manufacturer's protocol. The absorbance at 490 nm was measured using a HP845 spectrometer (Hewlett-Packard).

Quantitative Real-Time Polymerase Chain Reaction (Q-PCR). After 4 weeks of culturing, the hMSCs were lysed, and total RNAs were extracted from the hMSCs using RNeasy Mini Kit (Qiagen). The total RNAs were converted to cDNAs using reverse transcriptase and random primers (ImProm-II Reverse Transcription System, Promega) according to manufacturer's protocol. The identical amount of extracted total RNA (1 μg) in each samples was used in cDNA synthesis. The synthesized cDNAs were used in qPCR using a 7300 Real Time PCR system (Applied Biosystems). The information of the primers is shown in Table S1 in Supporting Information. The relative amount of mRNA expression of interest was normalized by that of β-actin and expressed as a fold change. The relative gene expression was evaluated by comparative cycle-threshold method. The expression level of the mRNAs of hMSCs cultured on the aligned CNT networks was normalized by that on the randomly oriented CNT networks.

Acknowledgment. This work was supported by NRF grant (No. 2011-0000390) and the Conversing Research Center Program (No. 2010-K000683). S.H. acknowledges the support of the Happy Tech. program (No. 20100020821) and the WCU program (R31-2010-000-10032-0). K.Y.B. acknowledges the support of the National Research Foundation of Korea Grant funded by the Korean Government (No.2010-0029418).

Supporting Information Available: Experimental methods to assemble CNTs in an aligned and a randomly oriented formation, supplementary optical microscope images, schematic diagrams showing plausible mechanism for the alignment of hMSCs along the aligned CNTs, and supplementary table showing the information of the primers used in the qPCR experiments. This material is available free of charge *via* the Internet at http://pubs.acs.org.

REFERENCES AND NOTES

1. Pittenger, M. F.; Mackay, A. M.; Beck, S. C.; Jaiswal, R. K.; Douglas, R.; Mosca, J. D.; Moorman, M. A.; Simonetti, D. W.; Craig, S.; Marshak, D. R. Multilineage Potential of Adult Human Mesenchymal Stem Cells. *Science* **1999**, *284*, 143–147.
2. Wagers, A. J.; Weissman, I. L. Plasticity of Adult Stem Cells. *Cell* **2004**, *116*, 639–648.
3. Kolf, C. M.; Cho, E.; Tuan, R. S. Biology of Adult Mesenchymal Stem Cells: Regulation of Niche, Self-Renewal and Differentiation. *Arthritis Res. Ther.* **2007**, *9*, 204.
4. Discher, D. E.; Mooney, D. J.; Zandstra, P. W. Growth Factors, Matrices, and Forces Combine and Control Stem Cells. *Science* **2009**, *324*, 1673–1677.
5. Segers, V. F. M.; Lee, R. T. Stem-Cell Therapy for Cardiac Disease. *Nature* **2008**, *451*, 937–942.
6. Stappenbeck, T. S.; Miyoshi, H. The Role of Stromal Stem Cells in Tissue Regeneration and Wound Repair. *Science* **2009**, *324*, 1666–1669.
7. English, K.; French, A.; Wood, K. J. Mesenchymal Stromal Cells: Facilitators of Successful Transplantation?. *Cell Stem Cell* **2010**, *7*, 431–442.
8. Dvir, T.; Timko, B. P.; Kohane, D. S.; Langer, R. Nanotechnological Strategies for Engineering Complex Tissues. *Nat. Nanotechnol.* **2010**, *6*, 13–22.
9. Dalby, M. J.; Gadegaard, N.; Tare, R.; Andar, A.; Riehle, M. O.; Herzyk, P.; Wilkinson, C. D. W.; Oreffo, R. O. C. The Control of Human Mesenchymal Cell Differentiation Using Nanoscale Symmetry and Disorder. *Nat. Mater.* **2007**, *6*, 997–1003.
10. Oh, S.; Brammer, K. S.; Li, Y.; Teng, D.; Engler, A. J.; Chien, S.; Jin, S. Stem Cell Fate Dictated Solely by Altered Nanotube Dimension. *Proc. Natl. Acad. Sci. U.S.A.* **2009**, *106*, 2130–2135.
11. Dang, J. M.; Leong, K. W. Myogenic Induction of Aligned Mesenchymal Stem Cell Sheets by Culture on Thermally Responsive Electrospun Nanofibers. *Adv. Mater.* **2007**, *19*, 2775–2779.

12. Lee, M. R.; Kwon, K. W.; Jung, H.; Kim, H. N.; Suh, K. Y.; Kim, K.; Kim, K. S. Direct Differentiation of Human Embryonic Stem Cells into Selective Neurons on Nanoscale Ridge/Groove Pattern Arrays. *Biomaterials* **2010**, *31*, 4360–4366.
13. Xie, J.; Willerth, S. M.; Li, X.; Macewan, M. R.; Rader, A.; Sakiyama-Elbert, S. E.; Xia, Y. The Differentiation of Embryonic Stem Cells Seeded on Electrospun Nanofibers into Neural Lineages. *Biomaterials* **2009**, *30*, 354–362.
14. Yim, E. K. F.; Darling, E. M.; Kulangara, K.; Guilak, F.; Leong, K. W. Nanotopography-Induced Changes in Focal Adhesions, Cytoskeletal Organization, and Mechanical Properties of Human Mesenchymal Stem Cells. *Biomaterials* **2010**, *31*, 1299–1306.
15. Zhu, B.; Lu, Q.; Yin, J.; Hu, J.; Wang, Z. Alignment of Osteoblast-like Cells and Cell-Produced Collagen Matrix Induced by Nanogrooves. *Tissue Eng.* **2005**, *11*, 825–834.
16. Weiner, S.; Traub, W.; Wagner, H. D. Lamellar Bone: Structure-Function Relations. *J. Struct. Biol.* **1999**, *126*, 241–255.
17. Lamers, E.; Frank Walboomers, X.; Domanski, M.; te Riet, J.; van Delft, F. C.; Luttge, R.; Winnubst, L. A. J. A.; Gardeniers, H. J. G. E.; Jansen, J. A. The Influence of Nanoscale Grooved Substrates on Osteoblast Behavior and Extracellular Matrix Deposition. *Biomaterials* **2010**, *31*, 3307–3316.
18. Tay, C. Y.; Gu, H. G.; Leong, W. S.; Yu, H. Y.; Li, H. Q.; Heng, B. C.; Tantang, H.; Loo, S. C. J.; Li, L. J.; Tan, L. P. Cellular Behavior of Human Mesenchymal Stem Cells Cultured on Single-Walled Carbon Nanotube Film. *Carbon* **2010**, *48*, 1095–1104.
19. Baik, K. Y.; Park, S. Y.; Heo, K.; Lee, K. B.; Hong, S. Carbon Nanotube Monolayer Cues for Osteogenesis of Mesenchymal Stem Cells. *Small* **2011**, *7*, 741–745.
20. Kam, N. W. S.; Jan, E.; Kotov, N. A. Electrical Stimulation of Neural Stem Cells Mediated by Humanized Carbon Nanotube Composite Made with Extracellular Matrix Protein. *Nano Lett.* **2008**, *9*, 273–278.
21. Namgung, S.; Kim, T.; Baik, K. Y.; Lee, M.; Nam, J. M.; Hong, S. Fibronectin-Carbon Nanotube Hybrid Nanostructures for Controlled Cell Growth. *Small* **2011**, *7*, 56–61.
22. LeMieux, M. C.; Roberts, M.; Barman, S.; Jin, Y. W.; Kim, J. M.; Bao, Z. Self-Sorted, Aligned Nanotube Networks for Thin-Film Transistors. *Science* **2008**, *321*, 101–104.
23. Mogilner, A.; Rubinstein, B. The Physics of Filopodial Protrusion. *Biophys. J.* **2005**, *89*, 782–795.
24. Condeelis, J. Life at The Leading Edge: The Formation of Cell Protrusions. *Annu. Rev. Cell Biol.* **1993**, *9*, 411–444.
25. Peskin, C. S.; Odell, G. M.; Oster, G. F. Cellular Motions and Thermal Fluctuations: The Brownian Ratchet. *Biophys. J.* **1993**, *65*, 316–324.
26. Gardel, M. L.; Schneider, I. C.; Aratyn-Schaus, Y.; Waterman, C. M. Mechanical Integration of Actin and Adhesion Dynamics in Cell Migration. *Annu. Rev. Cell Dev. Biol.* **2010**, *26*, 315–333.
27. Kilian, K. A.; Bugarija, B.; Lahn, B. T.; Mrksich, M. Geometric Cues for Directing The Differentiation of Mesenchymal Stem Cells. *Proc. Natl. Acad. Sci. U.S.A.* **2010**, *107*, 4872–4877.
28. Bhadriraju, K.; Yang, M.; Alom Ruiz, S.; Pirone, D.; Tan, J.; Chen, C. S. Activation of ROCK by RhoA Is Regulated by Cell Adhesion, Shape, and Cytoskeletal Tension. *Exp. Cell Res.* **2007**, *313*, 3616–3623.
29. McBeath, R.; Pirone, D. M.; Nelson, C. M.; Bhadriraju, K.; Chen, C. S. Cell Shape, Cytoskeletal Tension, and RhoA Regulate Stem Cell Lineage Commitment. *Dev. Cell* **2004**, *6*, 483–495.
30. Wozniak, M. A.; Chen, C. S. Mechanotransduction in Development: A Growing Role for Contractility. *Nat. Rev. Mol. Cell Biol.* **2009**, *10*, 34–43.
31. Leucht, P.; Kim, J. B.; Currey, J. A.; Brunski, J.; Helms, J. A. FAK-Mediated Mechanotransduction in Skeletal Regeneration. *PLoS One* **2007**, *2*, e390.
32. Salasznyk, R. M.; Klees, R. F.; Williams, W. A.; Boskey, A.; Plopper, G. E. Focal Adhesion Kinase Signaling Pathways Regulate The Osteogenic Differentiation of Human Mesenchymal Stem Cells. *Exp. Cell Res.* **2007**, *313*, 22–37.
33. Huang, C. H.; Chen, M. H.; Young, T. H.; Jeng, J. H.; Chen, Y. J. Interactive Effects of Mechanical Stretching and Extracellular Matrix Proteins on Initiating Osteogenic Differentiation of Human Mesenchymal Stem Cells. *J. Cell. Biochem.* **2009**, *108*, 1263–1273.
34. Gilmore, A.; Romer, L. Inhibition of Focal Adhesion Kinase (FAK) Signaling in Focal Adhesions Decreases Cell Motility and Proliferation. *Mol. Biol. Cell* **1996**, *7*, 1209–1224.